www.czasopisma.pan.pl PAN www.journals.pan.pl

ARCHIVES of FOUNDRY ENGINEERING

VERSITA

DOI: 10.2478/v10266-012-0104-z

ISSN (2299-2944)
Volume 12
Issue 4/2012

Published quarterly as the organ of the Foundry Commission of the Polish Academy of Sciences

39 – 46

Inoculation Effects of Cast Iron

E. Fraś, M. Górny*
AGH - University of Science and Technology,
Faculty of Foundry Engineering, Kraków, Poland
*Corresponding author. E-mail address: mgorny@agh.edu.pl

Received 19.06.2012; accepted in revised form 03.09.2012

Abstract

The paper presents a solidification sequence of graphite eutectic cells of A and D types, as well as globular and cementite eutectics. The morphology of eutectic cells in cast iron, the equations for their growth and the distances between the graphite precipitations in A and D eutectic types were analyzed. It is observed a critical eutectic growth rate at which one type of eutectic transformed into another. A mathematical formula was derived that combined the maximum degree of undercooling, the cooling rate of cast iron, eutectic cell count and the eutectic growth rate. One type of eutectic structure turned smoothly into the other at a particular transition rate, transformation temperature and transformational eutectic cell count. Inoculation of cast iron increased the number of eutectic cells with flake graphite and the graphite nodule count in ductile iron, while reducing the undercooling. An increase in intensity of inoculation caused a smooth transition from a cementite eutectic structure to a mixture of cementite and D type eutectic structure, then to a mixture of D and A types of eutectics up to the presence of only the A type of eutectic structure. Moreover, the mechanism of inoculation of cast iron was studied.

Keywords: Cast iron, Solidification, Inoculation, Structure, Eutectic cells

1. Introduction

Cast iron is the most important and most widely used casting alloy and its inoculation phenomenon was discovered in 1920 [1] and patented by Meeh in 1924 [2]. There are many studies on this phenomenon, which are summarized and analyzed in [3]. Elements such as Ba, Ca and Sr, which are usually introduced to a bath in ferrosilicon, are the most important inoculants of cast iron. Ferrosilicon that contains these elements is treated as a complex inoculant.

The purpose of this study were to analyze the inoculation effects and explain the inoculation mechanism of cast iron.

2. Solidification of graphite eutectic

After undercooling below the graphite eutectic equilibrium temperature, T_r, in the liquid alloy, graphite nuclei are created that take the form of rosettes during growth. On the concave surface of graphite rosettes, an austenite nucleates and surrounds the central part of the rosette, rising along its branches and leading to the creation of eutectic cells. From each nucleus, a single eutectic cell is formed. Therefore, the number of nuclei also represents the number of eutectic cells. In ductile iron, each graphite nucleus gives rise to a single graphite nodule. As the solidification process continues, the austenite shell nucleates directly on the graphite nodule and the eutectic transformation begins. Eutectic cells may contain a lot of nodules. Thus, in ductile iron, the number of nuclei can be identified only by the number of graphite nodules rather than the number of eutectic cells.

3. Solidification of cementite eutectic

After undercooling of cast iron below the cementite eutectic equilibrium temperature, T_c, in the liquid alloy, cementite nuclei are created that take the form of plates during growth. On this

plate, the austenite nucleates and grows in a dendritic form to cover the cementite. A common solidification front of the eutectic structure is created. During its growth, plate-to-fiber transition of cementite takes place and a cell of cementite eutectic is formed. In the central part of the cell, cementite takes the form of plates, while in the periphery, it assumes the form of fibers.

4. Morphology of eutectic cells

In a typical grey cast iron with flake graphite, there are two types of eutectic structures.

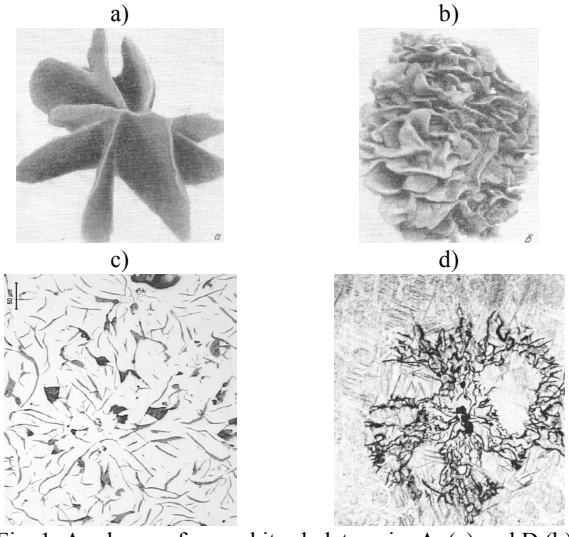

Fig. 1. A scheme of a graphite skeletons in A (a) and D (b) types of eutectic cells, microphotographs of cross sections of cells: with A type of eutectic formed at small undercooling (with low growing rate) (c) and with D type formed at high undercooling (with high growing rate) (d)

The A type of eutectic cells are formed at a low degree of undercooling, while the D type is formed at a high degree of undercooling. The appearance of skeletons in the graphite eutectic cells of A and D types are shown in Fig. 1a,b while microphotographs of their cross–sections are given in Fig. 1c, d. The skeleton of an A type of eutectic structure exhibits a small number of crystallographic errors of graphite crystal [5] and consequently, is poorly branched (Fig. 1a). On the other hand, the skeleton of a D type has a large number of crystallographic errors and is therefore much more branched.

5. Cell growth rate

The theory of eutectic growth [4] gives the general equation that combines the eutectic growth rate, u, with the degree of undercooling, ΔT.

$$u = \mu \Delta T^2 \qquad (1)$$

where μ - is the growth coefficient of eutectic cell.

The value of a growth coefficient for the eutectic cells with flake graphite depends on the chemical composition of the iron and is given in [6]. Therefore, for the cast iron containing 2% of Si, the equation (1) takes the following form:

$$u = 1{,}7\,10^{-6}\,\Delta T^2 \text{ ;cm/s} \qquad (2)$$

You may notice that the higher the degree of undercooling, the higher the cell growth rate.

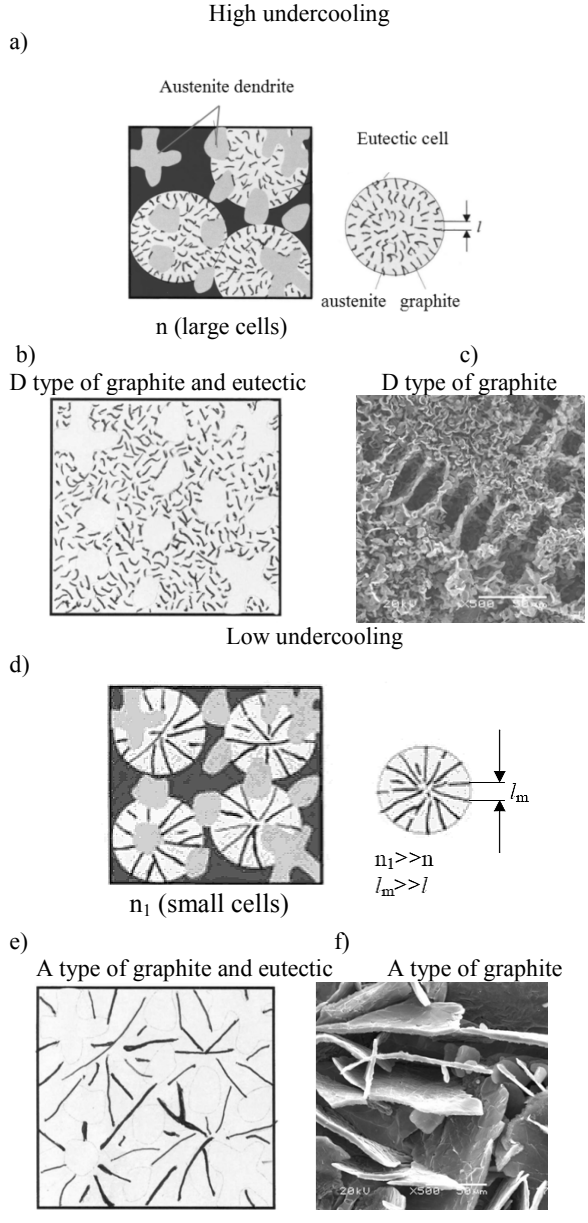

Fig. 2. Schemes of solidification of hypereutectic cast iron and interfacial distances between graphite precipitations (a, d), schemes of A and D type of eutectics (b, e) appearance of graphite of A and D type in scanning electron microscopy (c,f)

6. Interfacial distance

Interfacial distance λ is the distance between the branches of a continuous skeleton of graphite in the eutectic cell, which is observed on metallographic specimens (Fig. 2a and 2c show A and D types, respectively). The distance is much lower in the D type than in the A type.

The theory of eutectic growth [4] indicates that the interfacial distance in eutectic depends on their growth rate. According to the study [7], the interfacial distance can be determined from the following equations:

A type eutectic

$$\lambda = 136.8\, u^{-0,50} \quad ; \quad \mu m \tag{3}$$

D type eutectic

$$\lambda = 16,1\, u^{-0,25} \quad ; \quad \mu m \tag{4}$$

The graphs of these equations indicate a discontinuity within the interface distance between the A and D types of graphite eutectic structure (Fig. 3).

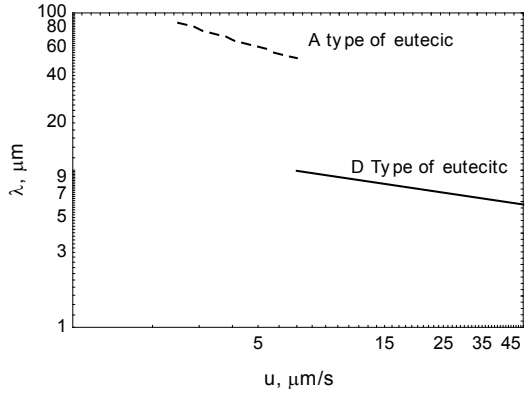

Fig. 3. Influence of growth rate on interfacial distance

From Fig. 3, there is a critical velocity growth range (around 7 to 10 μm/s) at which the interval change occurs within the interface distance.

7. Eutectic transformation in cast iron

In the fundamental theoretical work of [8] studying the relationship between free energy and eutectic growth rate, a critical growth rate of eutectic was demonstrated, called the transition rate, at which one type of eutectic is transformed into another. This general principle of energy, confirmed by the experimental studies of cast iron [2, 9], indicates that the transformation rate of the A type into the D type of a graphite eutectic structure amounts to u_{kr} = 1 ÷ 30 μm/s.

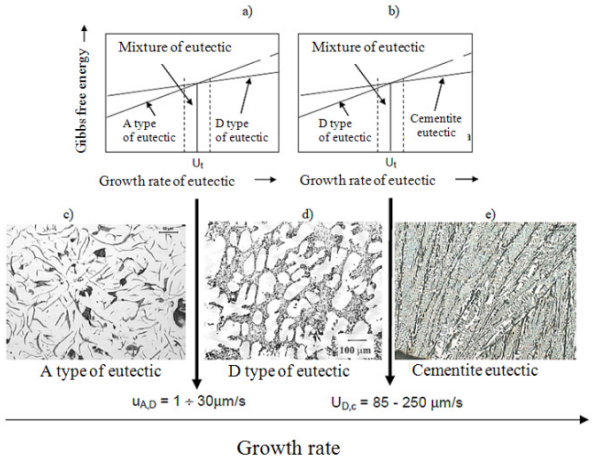

Fig.4. Influence of growth rate on free energy of eutectics (a,b); $u_{A,D}$ – trasformation rate of A to D type of eutectic, $u_{D,C}$ - trasformation rate of D type to cementite eutectic, microstructures (c,d,e) of A, D and cementite eutectics, respectively; values of transformation rates deal with pure Fe-C alloys

Below this rate range, the A type is formed since it has the lowest free energy, while above this range, the D type is produced, because its free energy is lower than that of the A type (Fig. 4a). Similarly, there is an experimentally determined rate range for the graphite-cementite eutectic transition ($u_{D,c}$ = 85 ÷ 250 μm/s) [9]. Above this rate range, cementite eutectic is formed because its free energy is lower than that for the D type of eutectic (Fig. 4b). Near the transformation range, the "smooth" transition of one type of eutectic into another through the eutectic mixture of different proportions (Fig. 5) is observed.

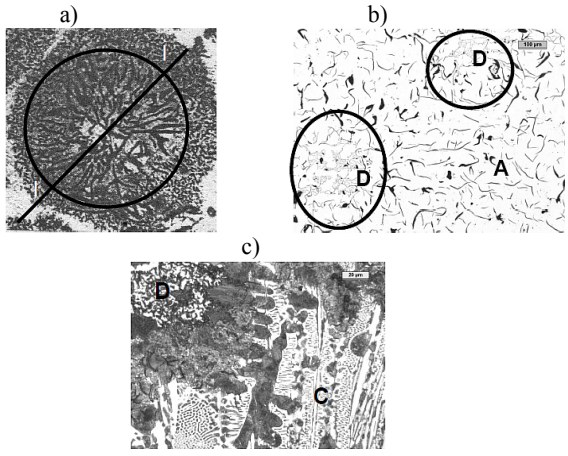

Fig.5 (a) Eutectic cell; central zone of A type of eutectic, outer zone of D type of eutectic, (b) appearance of cell cut by plane I-I and (c) mixture of D type and cementite eutectics formed close to transformation rate $u_{D,C}$ (Fig.4)

8. Number of eutectic cells

The number of eutectic cells in cast iron, N, varies in a wide range (e.g., Fig. 6c). The formation of the D type of eutectic is associated with a relatively low number of cells, while a high number is linked to the A type [10].

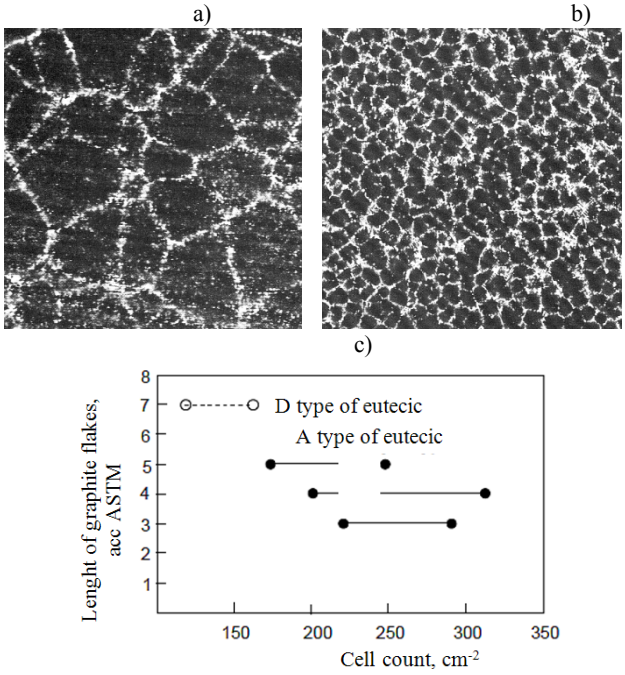

Fig. 6. Eutectic cell in cast iron (a, b) and influence of cell count and type of eutectic on graphite flake length, according to ASTM Standard (c)

9. Chilling tendency

A measure of the chilling tendency of cast iron is the fraction of the cementite eutectic structure in the standard casting, usually in the form of a wedge (Fig. 10).

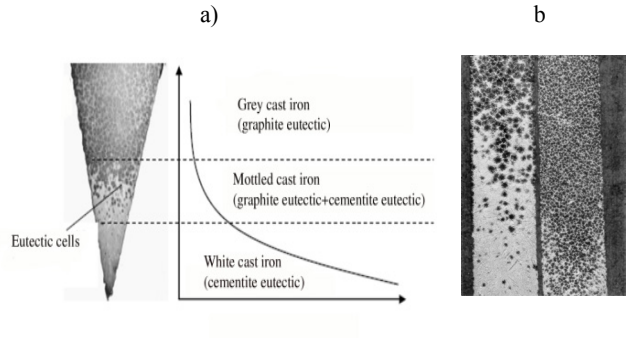

Fig. 7. Wedge for chilling tendency test (cementite eutectic formation) with cooling rate along its height (a), influence of cell count on the chills (b)

The cooling rate along with the height of the wedge is shown in Fig. 7b. It can be seen that there is a range of cooling rates (and thus the growth rate of cells) at which the transformation from graphite (grey cast iron) to cementite (white cast iron) eutectic via the eutectic mixture (mottled cast iron) occurs.

10. Calculations

Calculations comprised the uninoculated and inoculated cast iron having the same chemical composition (C = 3.16%; S i= 2.08%; P = 0.091%).

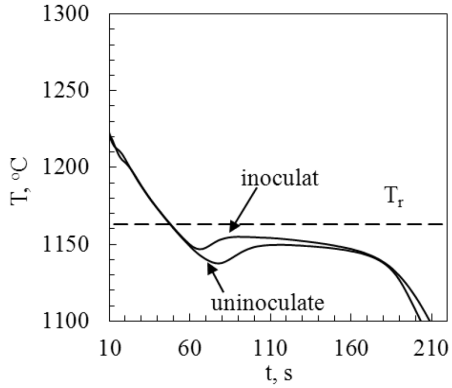

Fig. 8. Cooling curves of cast irons

From the cooling curves (Fig. 8), an average cooling rate was determined at temperature, T_r (T_r = 1153.9 + 5.25Si-14.88P =1164.4 °C), amounting to Q = 3.1 °C/s. From the metallographic images, the following parameters were determined: the number of eutectic cells N = 5011 cm^{-3} and N = 42404 cm^{-3} and the iinterfacial distance λ = 14 μm and λ = 53 μm for uninoculated and inoculated cast iron, which correspond to the D and A type of eutectics, respectively.

Degree of undercooling

Based on [11], taking into account equation (1) and the heat balance of the heat generated during solidification and the heat flowing into the mold, the general and the missing equation for the degree of undercooling of an eutectic alloy can be derived:

$$\Delta T_m = \left(\frac{4\, c_{ef}\, Q^3}{\pi^3 f_l\, \Delta H_e\, N\, \mu^3} \right)^{1/8} \tag{5}$$

where:
Q - cooling rate of alloy,
c_{ef} - specific heat of austenite,
ΔH_e - latent heat of graphite eutectic,
N - number of eutectic cells per unit volume,
μ - growth coefficient of eutectic cell.

After the adoption of previously indicated data and c_{ef} =15.2 J/(cm^3 °C) and ΔH_e = 2028.8 J/cm^3, the maximum degree of undercooling was calculated (Fig. 8) for:

uninoculated cast iron

$$\Delta T_m = \left[3{,}1^3 \frac{4\ 15{,}2}{0{,}74\,\pi^3\ 2028\ 5011\ (1{,}7\ 10^{-6})^3} \right]^{1/8} = 33{,}5\ ^{\circ}C \qquad (6)$$

inoculated cast iron

$$\Delta T_m = \left[3{,}1^3 \frac{4\ 15{,}2}{0{,}74\,\pi^3\ 2028\ 42404\ (1{,}7\ 10^{-6})^3} \right]^{1/8} = 25{,}6\ ^{\circ}C \qquad (7)$$

These values are comparable to the values determined on the basis of cooling curves (ΔT_m = 24.2°C and ΔT_m = 32.2°C; Fig. 8)

Cell growth rate

Taking into account the received values of the degree of undercooling and equations (2), (6) and (7), we calculated the cell growth rate at the maximum degree of undercooling ΔT_m for:

uninoculated cast iron

$$u = 1{,}7\,10^{-6}\ (33{,}5)^2 = 19{,}7\ \ \mu m/s \qquad (8)$$

inoculated cast iron

$$u = 1{,}7\,10^{-6}\ (25{,}6)^2 = 11{,}1\ \ \mu m/s \qquad (9)$$

Fig. 5 shows that the transformation rate of the eutectic transition from the A type to the D type was about 10 μm/s. The calculated transformation rate was in the range shown in Fig. 4, where there are two eutectic mixtures. The calculations show that in the inoculated cast iron, there is a greater tendency to the formation of the A type (lower growth rate) than in the uninoculated cast iron, where the higher growth rate indicates a greater tendency for the formation of the D type. This is confirmed by the microstructures in Fig. 9.

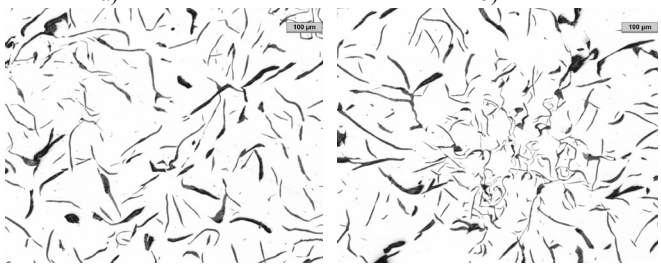

Fig. 9. A type of eutectic in inoculated cast iron and mixture of A type and D type of eutectics in uninoculated cast iron

Interfacial distance

After taking into account the calculated growth rate of cells (eq. (8) and (9)) based on equations (3), (4), (8) and (9), the interfacial distance can be calculated for:

A type of eutectic

$$\lambda = 136{,}8\,(11{,}1)^{-0{,}50} = 41{,}1\ \ \mu m \qquad (10)$$

D type of eutectic

$$\lambda = 16{,}1\ (19{,}7)^{-0{,}25} = 7{,}7\ \ ;\mu m \qquad (11)$$

The calculated ratio of interfacial distance of the A to the D type is 5.3 and is close to an experimentally specified value of 3.8 (ASTM A247-47). It is worth noting that these values are very similar to the eutectic in uninoculated and inoculated Al-Si alloy (about 5).

The temperature of transformation and the transformational number of cells

From equation (5), it can be seen that an increasing number of cells causes a reduction in the degree of undercooling of cast iron and according to equation (1), reduces the growth rate of eutectic cells. Calculations show that the cell growth rate can vary within the range of about 10 μm/s for strongly inoculated cast iron (50 000 cells/cm^3) to about 160 μm/s for the mottled iron, which is the base iron for the inoculation (1 cell/cm^3). They cover, therefore, the whole range of the transformation rates shown in Fig. 4, in which there are transitions: A □ (D+A) □ D□ (D+cementite)□ cementite.

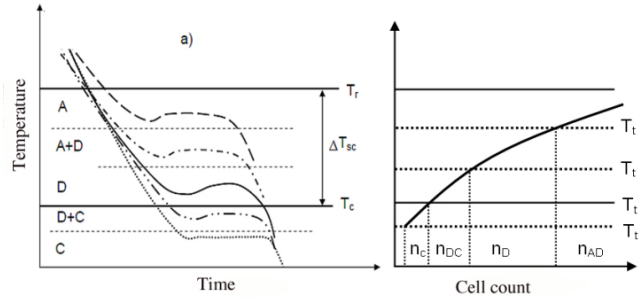

Fig. 10. (a) Cooling rate of cast iron and transformation temperature T_t of A to D type of eutectic; A to (A+D); (A+D) to D; D to (D+C) and (D+C) to C , also (b) influence of cell count on transformation temperature of eutectics

The analysis of equations (1) and (5) show that different transformation rates can be attributed to different transition temperatures, T_t, and transformational number of cells, N_t, at which one type of eutectic structure transforms into another. This is shown in Fig. 10, which displays the cooling curves of cast iron, as well as in the schematic diagram of equation (5) and the transformation temperature and transformational number of cells. The transformational number, n_t, and thus also the transition temperature, T_t, divided the solidification range of cast iron (Fig. 10) into five areas. In the first one, with a large number of cells and a small degree of undercooling, the A type was formed. In the second area, with a fewer number of cells and a higher degree of undercooling, a mixture of A and D types was formed, while in the third area, the D type of eutectic structure was created. The fourth area comprised a mixture of cementite and the D type, and the fifth, only cementite eutectic. An increase in the efficiency of inoculation was accompanied by a growing number of cells (Fig. 10b). If the number of cells exceeded the number of

transformation of n_{AD} (Fig. 10b), we obtained only the A type of eutectic structure, if the number of cells exceeded the number of transformation of n_D - a mixture of A and D types of eutectic, etc.

The transition temperatures, T_t depends also on chemical composition, especially on sulphur concentration in cast iron. Sulphur influences the A to D transition temperature ($T_t = T_{AD}$) which is shown in Fig. 11. From this figure results that as sulphur content increses an A type of graphite expands. At very low contents of sulphur an inoculation process lift eutectic transformation temperature and the number of eutectic grains but does not change the graphite transition of D type in A. Only after exceeding the sulphur content in cast iron over the level of 0.04-0.05% inoculation process transforms the D-type graphite in A.

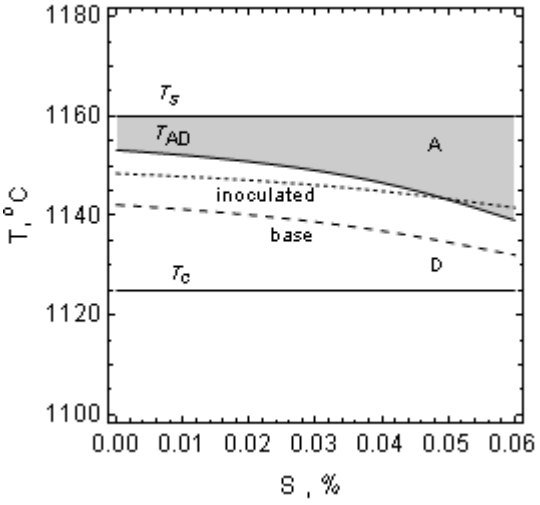

Fig. 11. Effect of sulphur on the transition temperature, $T_t = T_{AD}$

Chilling tendency

In [12], it was shown that the relative chilling tendency of cast iron can be determined by the equation:

$$CT_w = \frac{\Delta T_m}{\Delta T_{sc}} \tag{12}$$

The degree of undercooling ΔT_m gives equations (6) and (7) for the uninoculated and inoculated cast iron, respectively. The temperature range ΔT_{SC} = 48.1 and therefore, the calculated relative chilling tendency of uninoculated cast iron was 0.69 and higher than that for inoculated cast iron (0.53), which is consistent with the practice. Equations (5) and (12) indicate that the chilling tendency depends on the number of cells. The greater the number of cells, the smaller the degree of undercooling and consequently lower the chilling tendency. This confirms the image in Fig. 10b.

11. Secondary effects of inoculation

Matrix pearlitisation

As mentioned before, the inoculation treatment increases the probability of transformation from the D to the A type of eutectic structure. The D type is characterized by small distances between the graphite plates. During eutectoid transformation, the diffusion path of carbon in the austenite between the graphite flakes decreases and thus favors ferrite formation. In summary, reducing the number of cells in cast iron increases the probability of ferritic matrix formation. This is confirmed by the images in Fig. 15, which shows that a smaller number of cells (N_F = 620 mm^{-2}, Fig. 15 Ic) corresponds to the smaller distance between the graphite flakes (Fig. 15.Ia) and that ferrite is present in the matrix (Fig. 15.Ib). In the case of a high number of cells (N_F = 1659 mm^{-2}, Fig. 15.IIc), the distances between the graphite flakes are much larger (Fig. 15.IIa) and only pearlitic matrix is formed in the cast iron structure (Fig.15.II b), which increases the strength of cast iron.

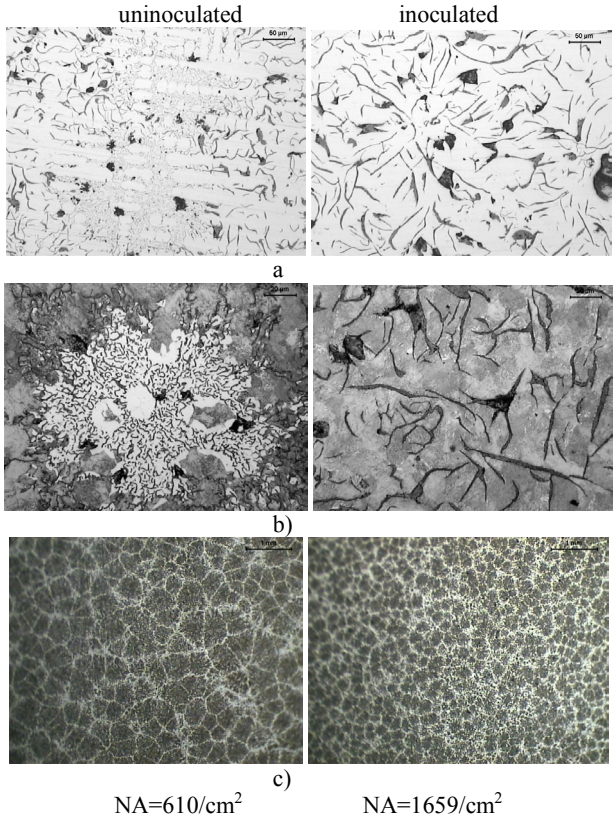

Fig.15. Influence of cell count (c) on interfacial distance between graphite flakes (a) and type of cast iron matrix (b).Bar with 14 mm diameter. a) Mag. 200 x unetched b) Mag. 500 x, Nital etched, c) Mag 10x, Stead etched

Shrinkage porosity

Inoculation treatment increasing the number of cells also increased the pressure generated during the solidification [13] and consequently the pre-shrinkage extension of cast iron. If the casting mold was not stiff enough, it caused increases in the shrinkage cavities (Fig. 16). If the inoculation process eliminated the cementite eutectic structure, it reduced the tendency for shrinkage cavities.

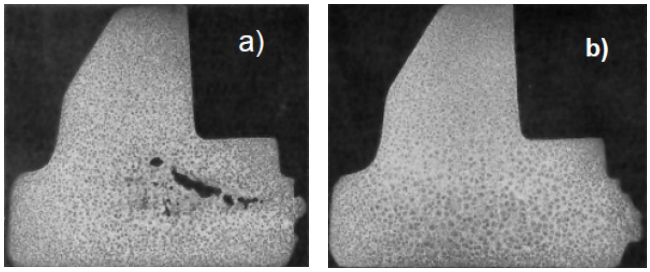

Fig.16 (a) Shrinkage cavities in cast iron with high cell count and (b) absence of shrinkage cavities in cast iron with low cell count

Mechanical properties

Inoculation treatment increased the number of cells, promoted the formation of pearlitic matrix and converted the D into the A type of eutectic structure. In addition, it decreased the chilling tendency, which can reduce the carbon equivalent of cast iron. All these increased the mechanical properties of cast iron.

12. Ductile iron

As in the case of cast iron with flake graphite, the introduction of inoculants into the liquid bath of ductile iron created additional substrates for graphite nucleation and hence, significantly increased the number of graphite nodules. This means that at a given rate of heat transfer flowing into the mold, the amount of heat generated increases during solidification and therefore, the degree of undercooling decreases. Very often, after spheroidisation treatment, ductile iron contains a mixture of cementite eutectic and graphite nodules (Fig. 17). The inoculation process of such iron raises the solidification temperature above the transformation temperature T_c (Fig. 1d) and thus, cementite eutectic disappears (Fig. 16b).

a) b)

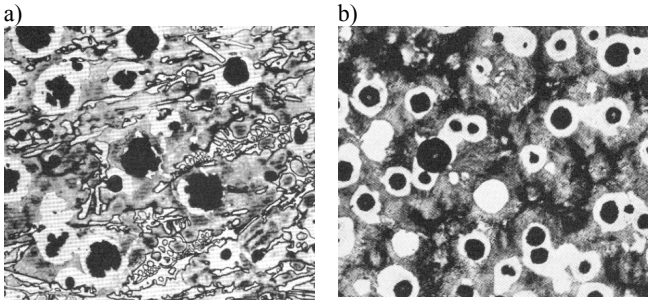

Fig. 17. Microstructure of ductile iron after spheroidization treatment (a) and after spheroidization and inoculation treatments (b)

13. Summary and inoculation mechanism of iron

From the above experimental study, the results from the inoculation process of cast iron answer the following questions: why, under the influence of inoculants, does the number of eutectic cells increase and the degree of undercooling decrease and why does the morphology of the eutectic structures change?

Eutectic cell growth starts from the primary crystal of graphite, which nucleates heterogeneously. Earlier studies [14, 15] have shown that after the introduction of calcium into the liquid bath, part of the calcium is consumed in local deoxidization and desulphurization processes, and the remainder of the calcium reacts with the carbon to give calcium carbide.

$$Ca + 2C = CaC_2 \tag{13}$$

Due to the similarity of lattice parameters of graphite and calcium carbide (Fig. 18), carbide particles act as additional substrates for graphite nucleation. Other simple inoculants such as strontium and barium act similarly. Increasing the number of substrates by introducing larger amounts of the inoculant into the liquid iron resulted in a greater number of eutectic cells, which is consistent with the foundry practice (Fig. 18b).

a)

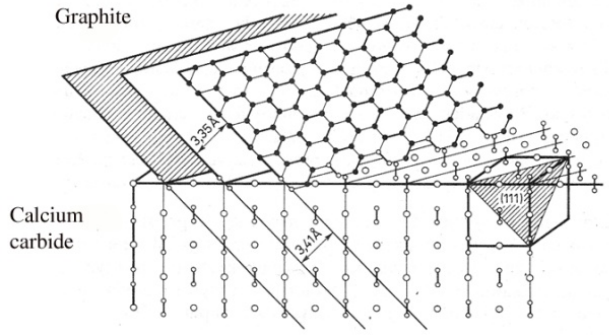

b)

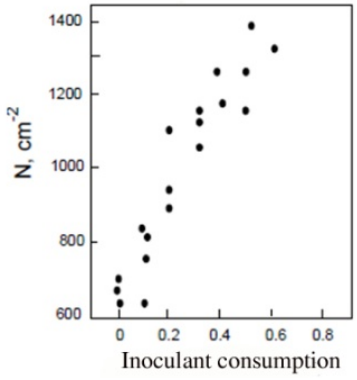

Fig. 18. Similarity of lattice parameters of graphite and calcium carbide (a) and influence of inoculant consumption (ferrosilicon with calcium additions) on cell count of graphite eutectic (b)

Increasing the number of cells means that at a given rate of heat transfer flowing into the mold, the amount of heat generated increases during solidification and therefore, the degree of undercooling decreases. As a result, the cell growth rate decreases (eq. (2)), while the interfacial distance (eq. (3) and (4)) increases. There is a critical growth rate of cells that corresponds to the transformational number of cells at which the eutectic

transformation occurs. As the inoculation efficiency increases, so does the number of cells (Fig.17b) and the following transformation occurs accordingly: C□(D+C)□D □ (D+A) □A. In ductile iron, (K+C) □K occurs (where C – cementite eutectic, D and A – type of eutectic structure, and K - nodular type of eutectic). In addition to the primary inoculation effects (i.e., increasing the number of eutectic cells and consequently, the structure of graphite), secondary effects also occur such as a reduction in the chilling tendency, a promotion of pearlitic matrix formation and changes in tendency for shrinkage cavities in cast iron.

Acknowledgments

This work was supported by Polish NCN Project N N508 621 140.

References

[1] Turner, T. (1920). *The Metallurgy of Cast iron*. Griffin Co.Ltd. London.
[2] Meehan, A. (1924). *US Patent 1 499 068*.
[3] Fraś, E. & Podrzucki, C. (1978). *Żeliwo modyfikowane*, Skrypt AGH, nr. 675, Kraków.
[4] Fraś, E. (2003). *Krystalizacja metali* WNT, Warszawa.
[5] Park, J. & Verhoven, J. (1996). Transitions between type A flake, type D flake and coral graphite eutectic structures in cast iron. *Metallurgical and Materials Transactions A*. 27A, 2740-2753.
[6] Fraś, E., Górny, M. & Lopez, H. (2005). The Transition from gray to white iron during solidification, part I – theoretical background. *Metallurgical and Materials Transactions A*. 36A, 3075-3082,
[7] Ohira, G., Sato, T. & Sayama, Y. (1974). *Eutectic growth unidierectionally solidified iron-carbon alloys*, Georgi Publishing Company, St. Shaporin, Switzeland, 296-313.
[8] Wołczyński, W. (2010). Lamella/Rod Transformation as described by the Criterion of Minimum Entropy Production. *International Journal of Thermodynamics*. 13 (2), 35-42.
[9] Magnin, P. & Kurz, W. (1988). Competitive growth of stable and metastable FE-C-X eutectics: Part II. Mechanism. *Metallurgical Transactions A*. 19A, 1965-1971.
[10] Fraś, E. & López, H. (2010). Eutectic cells and nodule count - an index of molten iron quality. *International Journal of Metalcasting*. Summer, 35-61.
[11] Fraś, E., Górny, M. & Lopez, H. (2007). Eutectic cell, chilling tendency and chill in flake graphite cast iron, part I – theoretical analysis. *Transactions of American Foundry Society*. 115, 435-451.
[12] Fraś, E., Górny, M. & Lopez, H. (2007). Eutectic cell, chilling tendency and chill in flake graphite cast iron, part III – thermal analysis. *Transactions of American Foundry Society*. 115, 476-480.
[13] Fraś, E. & López, H. (1994). Generation of internal pressure during solidification of eutectic cast iron. *AFS Transactions.* 102, 597-601.
[14] Lux, B. (1968). *Nucleation and graphite In Fe-C-Si alloys In Recent Research on Cast iron*, Gordon and Breach, New York, 241,
[15] Fraś, E., Lopez, H. & Podrzucki, C. (2000). The influence of oxygen on the inoculation process of cast iron. *Journal Cast Metal Research*. 13, 107-121.